

Modulation of the bonding-antibonding splitting in Te by coherent phonons

A. M.-T. Kim, C. A. D. Roeser, and E. Mazur

Harvard University, Division of Engineering & Applied Sciences and Department of Physics, 9 Oxford Street, Cambridge, Massachusetts 02138, USA

(Received 30 April 2003; published 22 July 2003)

We present femtosecond time-resolved measurements of the dielectric tensor of tellurium following intense photoexcitation. Strong impulsive photoexcitation of crystalline tellurium weakens the covalent bonds between atoms, which undergo coherent oscillations (at >3 THz) as they relax to new equilibrium positions. As this photoexcitation drives the lattice toward a band-crossing transition, we track the decrease and oscillation of the bonding-antibonding splitting. The reduction of the bonding-antibonding splitting exceeds the band gap for 100 fs, indicating a transient state with crossed bands.

DOI: 10.1103/PhysRevB.68.012301

PACS number(s): 78.47.+p

Ultrashort optical pulses of sub-100-fs duration enable the study of a great variety of ultrafast phenomena, among which are the generation and time-resolved detection of coherent phonons.¹ A number of experiments have been carried out and theories have been developed to understand the physics behind coherent phonons.^{2,3} It has been shown that Raman-active as well as infrared-active phonon modes can be coherently excited. Raman-active modes are excited via impulsive stimulated Raman scattering (ISRS) and infrared-active modes have been driven through the rapid screening of surface fields⁴ and the rapid buildup of a Demer field.⁵

A fundamentally different excitation mechanism called *displacive excitation of coherent phonons* (DECP) was proposed by Cheng *et al.* in 1991.⁶ The authors observed oscillations in the reflectivity of Te, Sb, Bi, and Ti_2O_3 at the frequency of the symmetry-preserving A_1 phonon mode in each material. Even though the A_1 mode is Raman active, ISRS is unlikely to be the generation mechanism because no other Raman-active modes were observed. The displacive excitation of coherent phonons is due to an impulsive weakening of the covalent bonds of the lattice following excitation of electrons from bonding valence-band states into antibonding conduction-band states.⁷ The lattice takes on a new equilibrium configuration due to the weakened covalent bonds and oscillates around it if the excitation pulse is short compared to the phonon period. The weakening of the lattice is isotropic, and thus only phonon modes that fully preserve the crystal symmetry are excited. For weak photoexcitation, the oscillatory frequency observed in tellurium is 3.6 THz,⁶ in agreement with continuous-wave Raman experiments.⁸ This model of a displacive excitation is further supported by experimental work on Te that demonstrates a softening of the A_1 mode for high excited carrier densities.⁹ Motivated by this finding, Tangney and Fahy performed *ab initio* calculations that revealed a linearly decreasing dependence of the A_1 phonon frequency on excited carrier density, in agreement with experiment.^{10,11} The calculations also indicated that intense photoexcitation of tellurium drives the lattice toward a band-crossing transition. Figure 1(a) shows the band structure of tellurium in its equilibrium, semiconducting configuration as calculated by density functional theory.¹² After an intense femtosecond pulse generates coherent phonons, theory predicts that the indirect gap decreases

as a result of the lattice displacement and that an indirect band-crossing transition occurs for a significant lattice displacement, as shown in Fig. 1(b).¹² Early experimental studies showed a decrease in the band gap due to pressure-induced lattice changes.^{13,14} However, no experimental study to date has monitored changes in the band structure of tellurium on the time scale of the ionic motion after impulsive photoexcitation.

In this paper we report the effects of displacively excited coherent phonons on the bonding-antibonding splitting in Te. We measured the time-resolved response of the dielectric

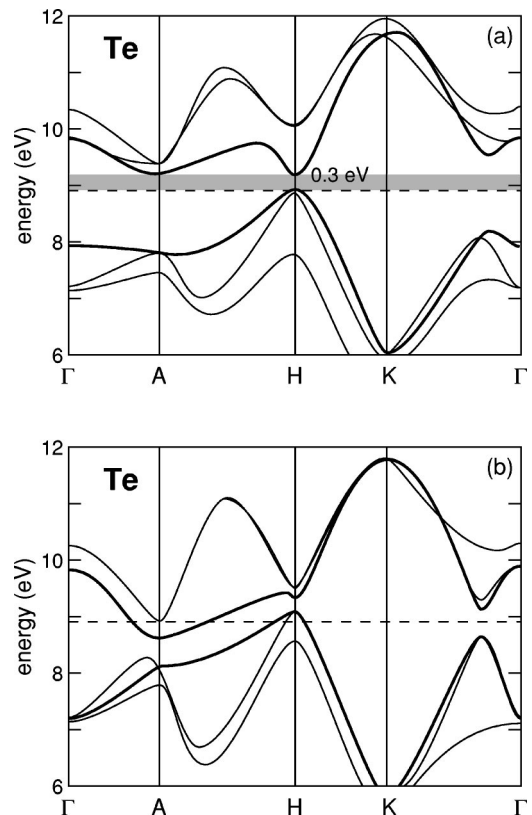


FIG. 1. Theoretical band structure of Te calculated using density functional theory (a) for the equilibrium lattice configuration and (b) for an atomic displacement of 0.018 nm along the A_1 phonon mode. After Ref. 12.

tensor of Te to strong photoexcitation. The measurements allow us to quantitatively track the bonding-antibonding splitting of the material. The data indicate a decrease in the bonding-antibonding splitting that is larger than the band gap, opening the possibility of an ultrafast reversible band-crossing transition.

We performed multiple-angle-of-incidence ellipsometry¹⁵ in a white-light pump-probe setup to measure the dielectric function over a broad photon energy range (1.8 – 3.4 eV) with 50-fs time resolution. Measuring reflectivity values at two angles of incidence allows extraction of the real and imaginary part of $\epsilon(\omega)$ by numerical inversion of the Fresnel reflectivity formulas. A Czochralski-grown single crystal of Te is excited with 800-nm pulses from a multi pass amplified Ti:sapphire system, producing 0.5-mJ, 35-fs pulses at a repetition rate of 1 kHz.¹⁶ The white-light (1.8 – 3.4 eV) probe is obtained by focusing a 1.55-eV laser pulse into a 2-mm-thick piece of CaF₂. To correct for dispersive stretching of this broadband probe pulse, we measure the chirp separately using two-photon-absorption¹⁷ and time-shift the data accordingly. We acquire reflectivity spectra using an imaging spectrograph and a fast charge-coupled-device (CCD) detector, enabling data acquisition at the 1-kHz repetition rate of the laser system. The detection system is calibrated so as to obtain absolute reflectivity values. The sensitivity to relative reflectivity changes is $\Delta R/R \leq 10^{-3}$. In all experiments, the excited area on the sample is significantly larger than the probed area — 500 μm vs 10 μm — to minimize the effects of lateral carrier-density inhomogeneity. Further details of our technique can be found elsewhere.^{18,19}

The tellurium crystal structure consists of three-atom-per-turn helices whose axes are arranged on a hexagonal lattice.²⁰ The A_1 phonon mode is a “breathing” mode of the lattice for which the helical radius changes but the interhelical distance and c -axis spacing remain constant, preserving crystal symmetry.

The uniaxial nature of Te requires that the dielectric tensor have two independent elements — an ordinary and an extraordinary one. Each of those elements has a real and an imaginary part, leading to four unknown quantities to be extracted from four reflectivity measurements. We performed two measurements with a p -polarized probe and with the c axis perpendicular to the plane of incidence and two with the same probe polarization, but with the c axis in the plane of incidence. The components of the dielectric tensor, $\epsilon_{\text{ord}}(\omega)$ and $\epsilon_{\text{ext}}(\omega)$, are determined using an extension of the Fresnel formulas that accounts for birefringence.^{21,22}

Figure 2 shows the values of $\epsilon_{\text{ord}}(\omega)$ and $\epsilon_{\text{ext}}(\omega)$ measured 500 fs before excitation. The size of the error bars is on the order of the size of the data points. The excellent agreement between the literature values measured by continuous wave (cw) ellipsometry,²³ represented by the solid and dashed lines, and the values obtained in our apparatus validates the technique.

Figure 3 shows the temporal evolution of $\epsilon_{\text{ord}}(\omega)$ after excitation with a fluence of 120 J/m². Following excitation, all features of both $\epsilon_{\text{ord}}(\omega)$ and $\epsilon_{\text{ext}}(\omega)$ shift to lower energies and oscillate, indicating the presence of coherent phonons. We measured the dielectric functions in 30-fs inter-

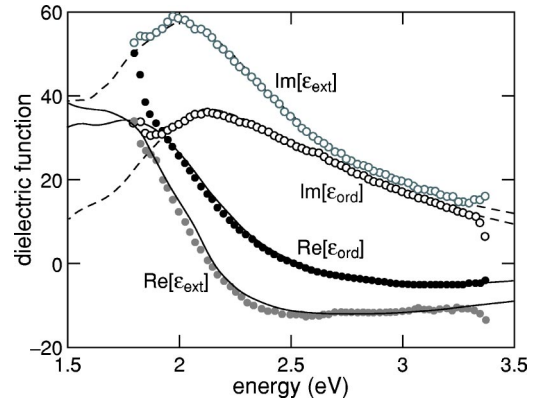


FIG. 2. Ordinary (black) and extraordinary (gray) part of the dielectric tensor of Te 500 fs before excitation with a fluence of 120 J/m². Open circles indicate the imaginary part and solid circles the real parts of $\epsilon(\omega)$. The solid and dashed curves show the real and imaginary parts of $\epsilon_{\text{ord}}(\omega)$ and $\epsilon_{\text{ext}}(\omega)$ from cw measurements (Ref. 23).

vals from –500 fs to 2.5 ps; the data can be animated to provide a movie of $\epsilon(\omega)$ that clearly shows the oscillatory behavior due to the coherent phonons.²⁴ As Fig. 3 shows, both the peak in $\text{Im}[\epsilon_{\text{ord}}(\omega)]$ and the zero of $\text{Re}[\epsilon_{\text{ord}}(\omega)]$ are significantly redshifted after excitation. At 220 fs, the redshift of $\epsilon_{\text{ord}}(\omega)$ is maximal. At 370 fs, approximately half a

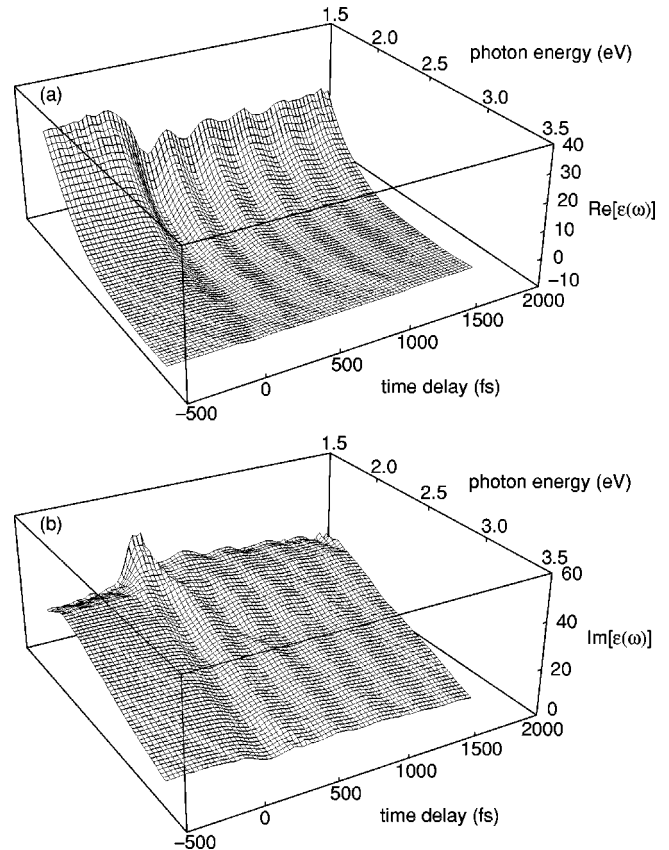


FIG. 3. Temporal evolution of (a) $\text{Re}[\epsilon_{\text{ord}}(\omega)]$ and (b) $\text{Im}[\epsilon_{\text{ord}}(\omega)]$ of Te following intense photoexcitation at a fluence of 120 J/m².

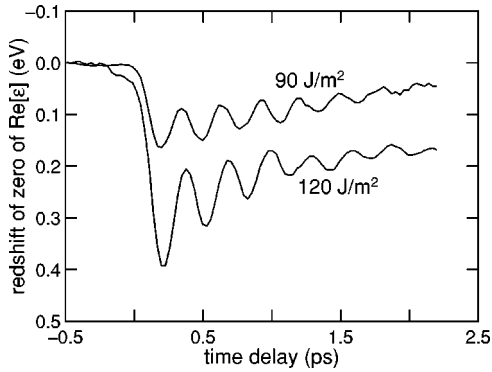


FIG. 4. Temporal evolution of the change in the zero of $\text{Re}[\epsilon_{\text{ord}}(\omega)]$ following excitations at 90 J/m^2 and 120 J/m^2 .

phonon period later, $\epsilon_{\text{ord}}(\omega)$ reaches another local extremum of its motion. The periodic lattice distortions continue to modulate the dielectric tensor for many picoseconds.

The oscillatory motion of $\epsilon(\omega)$ can clearly be seen in Fig. 4, which shows the transient behavior of the zero of $\text{Re}[\epsilon_{\text{ord}}(\omega)]$. We fit the traces of the zero of $\text{Re}[\epsilon(\omega)]$ to an overdamped oscillator driven by an exponentially decreasing offset from its initial position.⁷ The difference between the data and this fit yields just the oscillatory signal, and the Fourier transformation gives the frequency and a measure of the amplitude of the oscillations. Extrapolating our data to low excitation fluences, we determine the A_1 phonon frequency of Te to be 3.6 THz under weak photoexcitation, in agreement with previous experimental results.^{6,9} The slow exponential decay component of the traces in Fig. 4 can be attributed to the relaxation of the new equilibrium configuration of the Te lattice to the unexcited state due to carrier diffusion out of the probed region. This general scenario of highly photoexcited Te is in agreement with the previous experimental and theoretical work.^{6,7,9,11}

As Fig. 4 further shows, the offset and amplitude of the oscillations increase with excitation fluence, indicating an increase in both the shift of the equilibrium helical radius and the amplitude of the coherent phonon. A linear regression through the peak frequency data of the zero of $\text{Re}[\epsilon_{\text{ord}}(\omega)]$ shows that the A_1 phonon frequency softens with increasing excitation fluences at a rate of $-0.0025 \text{ THz per J/m}^2$, in agreement with previous reflectivity-based measurements.⁹ Performing the same analysis as described above with the $\epsilon_{\text{ext}}(\omega)$ data (not presented here) shows that the oscillations of $\epsilon_{\text{ext}}(\omega)$ are of smaller amplitude than those of $\epsilon_{\text{ord}}(\omega)$. This difference can be attributed to the fact that the A_1 mode oscillates in the ab plane of the crystal and $\epsilon_{\text{ord}}(\omega)$ describes the optical properties in that plane.

Because the zero of $\text{Re}[\epsilon(\omega)]$ corresponds to the bonding-antibonding splitting in a material,²⁵ Fig. 4 reflects the transient behavior of this bonding-antibonding splitting. As the figure shows, the bonding-antibonding splitting rapidly decreases, followed by an oscillation around a new equilibrium value that decays with time. Theoretical work has shown that the band structure of Te changes dramatically as the atoms move along the direction of the A_1 mode and that a band-crossing transition occurs when the helical radius in-

creases by about 6%,¹² requiring a photoexcited electron density of about 1.2% of valence electrons.¹⁰ Assuming strictly linear absorption, a pump fluence of 120 J/m^2 produces an excited carrier density of $4.8 \times 10^{21} \text{ cm}^{-3}$, corresponding to about 3% of valence electrons in Te. The observed decrease in the bonding-antibonding splitting indicates that the equilibrium helical radius increases upon excitation, driving the system toward a band-crossing transition.²⁶

At the highest pump fluence of 120 J/m^2 , the lattice displacement at 220 fs is so large that the reduction of the bonding-antibonding splitting reaches 0.4 eV, exceeding the 0.3-eV indirect band gap of Te for 100 fs. DFT calculations show that the modulation of the dielectric tensor due to lattice displacements along the A_1 mode is mostly attributable to a drop of the lowermost conduction band at the A point in the Brillouin zone.²⁸ Thus, the measured decrease of the zero of $\text{Re}[\epsilon_{\text{ord}}(\omega)]$ should be interpreted as a reduction of the energy of the conduction-band states around A by the same amount. The magnitude of this reduction suggests that the lowermost conduction band and the uppermost valence band cross (see Fig. 1). While a metallic (Drude-like) dielectric function is expected for a material with crossed bands, the dielectric function data at 220 fs do not show significant free carrier (Drude) contributions (see Fig. 3).

A metallic dielectric function will be seen when a large density of electrons in valence-band states of the H valley scatter into the conduction-band states of the A valley made accessible by the displacive excitation of the lattice and the resultant indirect band crossing. In the case of the data presented here, conduction-band states are accessible via scattering only near the peak displacement of the coherent phonons. Because electron-phonon scattering times in semiconductors are on the order of several hundred femtoseconds,² the time available for the redistribution of electrons is too short, preventing any metallic character from emerging before the ions move to smaller displacement and the conduction-band states become energetically inaccessible.

In conclusion, we measured the response of the dielectric tensor of Te to strong photoexcitation. Both the ordinary and extraordinary parts of $\epsilon(\omega)$ redshift to lower energy due to lattice displacements caused by bond weakening and oscillate due to the presence of displacively excited coherent phonons. The data allow us to directly track the bonding-antibonding splitting of the material. The magnitude of the decrease in the bonding-antibonding splitting and the absence of a metallic dielectric function suggest a transient state with crossed bands that is nonmetallic. When combined with the data presented here, theoretical calculations, similar to those in Ref. 10, of the dielectric tensor for various helical radii would reveal both the actual phonon amplitude as well as the degree of band crossing.

We gratefully acknowledge P. Grosse for providing single-crystal Te samples and P. Tangney, S. Fahy, H. Ehrenreich, N. Cholý, and E. Kaxiras for discussions. This work was supported by the National Science Foundation under Grant No. DMR-9807144.

- ¹S. DeSilvestri, J. G. Fujimoto, E. P. Ippen, E. B. Gamble, L. R. Williams, and K. A. Nelson, *Chem. Phys. Lett.* **116**, 146 (1985).
- ²J. Shah, *Ultrafast Spectroscopy of Semiconductors and Semiconductor Nanostructures* (Springer-Verlag, Berlin, 1996).
- ³R. Merlin, *Solid State Commun.* **102**, 207 (1997).
- ⁴G. C. Cho, W. Kutt, and H. Kurz, *Phys. Rev. Lett.* **65**, 764 (1990).
- ⁵T. Dekorsy, H. Auer, C. Waschke, H. J. Bakker, H. G. Roskos, and H. Kurz, *Phys. Rev. Lett.* **74**, 738 (1995).
- ⁶T. K. Cheng, J. Vidal, M. J. Zeiger, G. Dresselhaus, M. S. Dresselhaus, and E. P. Ippen, *Appl. Phys. Lett.* **59**, 1923 (1991).
- ⁷H. J. Zeiger, J. Vidal, T. K. Cheng, E. P. Ippen, G. Dresselhaus, and M. S. Dresselhaus, *Phys. Rev. B* **45**, 768 (1992).
- ⁸P. Grosse, *Die Festkörpereigenschaften von Tellur*, Vol. 48 of *Springer Tracts in Modern Physics* (Springer-Verlag, Berlin, 1969).
- ⁹S. Hunsche, K. Wienecke, T. Dekorsy, and H. Kurz, *Phys. Rev. Lett.* **75**, 1815 (1995).
- ¹⁰P. Tangney and S. Fahy, *Phys. Rev. Lett.* **82**, 4340 (1999).
- ¹¹P. Tangney and S. Fahy, *Phys. Rev. B* **65**, 054302 (2002).
- ¹²P. Tangney, Master's thesis, University College Cork, Ireland, 1998.
- ¹³J. Bardeen, *Phys. Rev.* **75**, 1777 (1949).
- ¹⁴F. A. Blum and B. C. Deaton, *Phys. Rev.* **137**, A1410 (1965).
- ¹⁵D. Beaglehole, *Proc. Phys. Soc. London* **85**, 1007 (1965).
- ¹⁶S. Backus, J. Peatross, C. P. Huang, M. M. Murnane, and H. C. Kapteyn, *Opt. Lett.* **20**, 2000 (1995).
- ¹⁷T. F. Albrecht, K. Seibert, and H. Kurz, *Opt. Commun.* **84**, 223 (1991).
- ¹⁸A. M.-T. Kim, Ph.D. thesis, Harvard University, 2001.
- ¹⁹C. A. D. Roeser, A. M.-T. Kim, J. P. Callan, L. Huang, E. N. Glezer, Y. Siegal, and E. Mazur, *Rev. Sci. Instrum.* **74**, 3413 (2003).
- ²⁰J. Donohue, *The Structures of the Elements* (Wiley, New York, 1974).
- ²¹L. P. Mosteller, Jr. and F. Wooten, *J. Opt. Soc. Am.* **58**, 511 (1968).
- ²²F. Wooten, *Appl. Opt.* **23**, 4226 (1984).
- ²³E. D. Palik, *Handbook of Optical Constants of Solids* (Academic Press, New York, 1985).
- ²⁴See EPAPS Document No. E-PRBMDO-68-056325 for a movie showing the oscillatory behavior due to the coherent phonons. A direct link to this document may be found in the online article HTML reference section. The document may also be reached via the EPAPS homepage (<http://www.aip.org/pubservs/epaps.html>) or from <ftp.aip.org> in the directory/epaps/. See the EPAPS homepage for more information.
- ²⁵W. A. Harrison, *Electronic Structure and the Properties of Solids: The Physics of the Chemical Bond* (Dover, New York, 1989).
- ²⁶This observation is in direct contrast to the conclusion reached in Ref. 27, where the authors suggest a decrease of the helical radius upon intense photoexcitation.
- ²⁷S. Hunsche, K. Wienecke, and H. Kurz, *Appl. Phys. A* **62**, 499 (1996).
- ²⁸N. Choly and E. Kaxiras (private communication).